

Mechanical Properties of Ferritic Stainless Steels at Elevated Temperature

Manninen, T. and Säynäjäkangas J.

Outokumpu Stainless Oy, Tornio Research Centre, FI-95490 Tornio Finland

Abstract

The elevated temperature mechanical properties have an important role in the fire safety design of structures. The reduction in mechanical properties is considered the primary element affecting the performance of steel structures under fire conditions. Ferritic stainless steels are low cost, price-stable, corrosion-resistant steels. These steels have a great potential for application in the construction industry. However, past research on design of stainless steel has been mainly focused on the austenitic and duplex grades. Therefore, the reduction of mechanical properties of ferritic stainless steels under fire conditions is largely unknown. In the present work, an extensive experimental research programme was carried out to investigate the mechanical properties of various ferritic stainless steels at temperatures up to 1000°C. The results were used to define strength retention factors for the studied ferritic stainless steel grades

1 Introduction

Ferritic stainless steels are low-cost, price-stable, corrosion-resistant steels. In contrast to austenitic grades, ferritic grades have low thermal expansion, high thermal conductivity and they are immune for chloride-induced stress-corrosion cracking (SCC). The ferritic grades are widely used in the automotive and household appliance sectors. Structural applications of these materials in the construction industry are, however, scarce.

One major barrier to the wider use of ferritic stainless steels in construction is the lack of relevant design guidance. Only one ferritic stainless steel grade 1.4003 is currently covered by the European design code [1,2]. Moreover, the grade 1.4003 is a structural ferritic stainless steel with only ~12% of chromium. Therefore, the corrosion resistance of 1.4003 is not comparable to that of most common austenitic grades. Ferritic grades with higher corrosion resistance are well established, but design values for these medium and high-chromium grades are not provided by the European design code.

Elevated temperature mechanical properties play an important role in the fire design of steel structures. Appropriate assessment of fire safety requires that the material response at elevated temperature can be predicted. However, past work on structural design with stainless steel has been mainly focused on the austenitic and duplex grades [3, 4, 5]. The reduction of mechanical properties of ferritic stainless steels under fire conditions is largely unknown. In the present work, an experimental research programme was carried out to investigate the mechanical properties of various ferritic stainless steels at temperatures up to 1000°C. The objective of the work was to derive the strength retention factors for ferritic stainless steel grades 1.4016, 1.4509, 1.4521 and 1.4621 in the temperature range between +20°C and +1000°C. Material from two European producers was used when available.

2 Experimental Procedures

2.1 Testing programme and test materials

Steady state tests were carried out for the ferritic stainless steel grades 1.4003, 1.4016, 1.4509, 1.4521 and 1.4621 in the temperature range between +20°C and +1000°C. The steel grade 1.4003 was included as a reference material. Material from two suppliers was tested for the grades 1.4016, 1.4509 and 1.4521. Transient state tests were performed on steel grades 1.4509 and 1.4521. Sixteen different load levels between 10% and 90% of the yield stress were used. A slow heating rate of 10°C/min was used in the transient tests.

The test materials were cold-rolled sheets in annealed condition by three European producers. The test pieces were cut in the rolling direction. The chemical compositions of studied materials are given in Table 1. The room-temperature mechanical properties of test materials in the rolling direction are given in Table 2. The measurements were carried out according to the standard EN ISO 6892-1 method A224.

The grades 1.4509, 1.4521 and 1.4621 are modern stabilized ferritic stainless steels. In these alloys, the interstitial carbon and nitrogen is bound by stabilizing elements such as Nb and Ti. Carbides and nitrides are precipitated depleting the solid solution of free carbon and nitrogen. The precipitated nitrides and carbides, stable at high temperature, act as barriers to dislocation motion, and inhibit grain boundary sliding and grain growth. Therefore, stabilized grades retain their strength at elevated temperature better than unstabilized ones. Stabilized grades are therefore commonly used for elevated temperature applications such as exhaust pipes.

Table 1 Chemical composition of test materials (wt%)

Grade	Supplier	Type	Identifier	C	Si	Mn	Cr	Ni	Mo	Ti	Nb	Cu	Al	N	KFF
1.4003	B	2B	4003-1	0.015	0.26	1.45	11.4	0.4	0.0	0.00	0.01	0.1	0.00	0.013	7.4
1.4016	A	2B	4016-1	0.023	0.36	0.46	16.3	0.2	0.0	0.01	0.01	0.1	0.01	0.028	14.8
1.4016	B	2B	4016-2	0.046	0.30	0.48	16.1	0.2	0.2	0.00	0.02	0.1	0.00	0.027	14.1
1.4509	A	2B	4509-1	0.017	0.55	0.45	17.8	0.2	0.0	0.14	0.49	0.0	0.05	0.018	19.3
1.4509	B	2B	4509-2	0.020	0.55	0.48	17.9	0.3	0.0	0.12	0.40	0.1	0.01	0.030	18.4
1.4521	A	2B	4521-1	0.011	0.48	0.44	17.7	0.3	2.0	0.17	0.43	0.1	0.00	0.016	26.6
1.4521	B	2B	4521-2	0.015	0.52	0.49	18.0	0.1	2.0	0.13	0.40	0.2	0.01	0.019	27.3
1.4521	B	2B	4521-3	0.012	0.48	0.49	17.9	0.2	2.0	0.13	0.39	0.2	0.01	0.023	27.0
1.4621	C	2R	4621-1	0.014	0.21	0.23	20.6	0.2	0.0	0.01	0.45	0.4	0.00	0.014	19.7

KFF = Ferrite Factor

Table 2 Room temperature mechanical properties of test materials measured in the rolling direction

Grade	Identifier	Thickness (mm)	Rp0,01 (N/mm ²)	Rp0,1 N/mm ²	Rp0,2 N/mm ²	Rp1,0 N/mm ²	Rt2,0 N/mm ²	Rm N/mm ²	Ag %	A80 %	A5 %
1.4003	4003-1	2.0	234	318	330	357	380	493	16.2	31.3	50.7
1.4016	4016-1	2.0	237	299	311	338	358	478	16.8	26.0	38.0
1.4016	4016-2	2.0	237	305	315	333	349	458	17.4	33.3	53.3
1.4509	4509-1	2.0	250	321	331	353	369	479	17.6	29.0	43.0
1.4509	4509-2	2.0	287	358	367	384	398	488	15.9	33.0	54.3
1.4521	4521-1	2.0	291	367	375	396	416	542	16.2	29.3	44.7
1.4521	4521-2	2.0	309	382	394	419	438	564	15.6	27.7	43.7
1.4521	4521-3	2.0	337	379	391	411	410	532	17.3	28.4	41.9
1.4621	4521-1	1.5	279	351	359	373	406	469	15.9	32.0	56.0

2.2 Test equipment

Steady state and transient state material testing was performed using a Zwick Z250/SW5A tensile testing machine with the capacity of 250kN. The tensile testing machine is equipped with a low temperature environmental chamber and a high temperature furnace. The environmental chamber can be used in the temperature range between 25°C and 550°C. For temperatures above 550°C, the high temperature furnace is used. The environmental chamber is a convection oven with temperature control in the convector unit. The high temperature furnace is heated with a three resistor zones. The temperature in each zone is controlled with a thermocouple connected to the Eurotherm 2416 controller unit. The sample elongation is measured using the Maytec side-entry extensometer with ceramic sensor arms. The tensile testing equipment belongs to accuracy class 1 and it is regularly calibrated according to the standards EN ISO 7500-1:2004 and EN ISO 9513:2002.

The piece geometry is shown in Fig. 1. This test piece geometry corresponds to the specifications for non-proportional test pieces in the standard ISO EN 10002-5 annex A. The test pieces were fabricated by machining. The original gauge length used for this type of test piece is $L_0 = 50\text{mm}$.

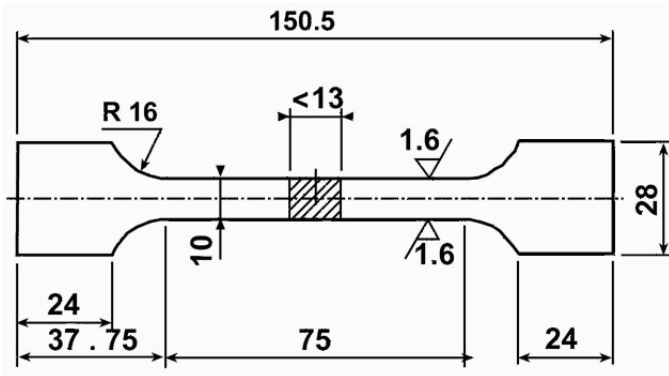


Figure 1 Test piece geometry.

2.3 Steady state test method

The steady state tests were performed at temperature intervals of 100°C between room temperature and 500°C and at temperature intervals of 50°C between 500°C and 1000°C. Two identical tests were carried out at each temperature. Occasionally, a third test carried out if there was a large disparity between the results. The test piece temperature in the oven was measured by means of three K-type thermocouples pressed to the surface of the test piece. The temperature of the test piece was controlled within the limits given by the testing standard EN ISO 10002-5. In the beginning of the test, the test piece was heated to the specified temperature and maintained at that temperature for 10 minutes before loading. The sample elongation was measured using a side-entry extensometer. The extensometer was reset to zero immediately before the onset of loading. The tests were carried out under strain control. The straining rate was 0.005 min⁻¹ in the first part of the test ($\epsilon \leq 1.5\%$) and 0.2 min⁻¹ thereafter.

2.4 Transient state test method

In the transient state tests, the load applied on the specimen is kept constant and the temperature is increased with a constant heating rate. The temperature and the elongation of the specimen are measured continuously during the test. The test is continued until the specimen fails or the target temperature of 1000°C is reached.

The transient state tests were carried out using the high temperature furnace. The heating rate was 10°C/min. The sample elongation was measured using a side-entry extensometer. The sample temperature was measured using three K-type thermocouples attached to the surface of the test piece. The anisothermal tests were conducted using sixteen evenly spaced stress levels between 10% and 90% of the room temperature yield stress. Two equal tests were performed at each stress level. A third test was performed if there was a large disparity between the results. The thermal expansion of the sample was measured using a small stress level of 3 MPa. The thermal elongation was subtracted from the results before calculation of retention factors.

Elastic strains were calculated using the elevated temperature elastic modulus values published by Outokumpu for steel grades 1.4509 and 1.4521. These values were measured by Katholieke Universiteit Leuven using the impulse excitation technique [6]. The experimental Young's modulus values are accurately described by the second order polynomial

$$E = E_0[-2.61 \times 10^{-7} \theta^2 - 2.87 \times 10^{-4} \theta + 1.0] \quad (1)$$

where θ (°C) is the steel temperature and $E_0 = 220 \text{ GPa}$.

3 Results

3.1 Steady state test results

The steady state test results for steel 4016-2 are shown in Fig. 2. The following distinct features stages can be identified in the stress-strain curves of this unstabilized grade:

- In the range $200^\circ\text{C} \leq T \leq 400^\circ\text{C}$, the strength of the material remains roughly constant despite of the increasing temperature. This behaviour can be attributed to dynamic strain aging (DSA). DSA is typical for materials, which have a BCC structure, and which contain interstitial carbon [7, 8]. Further evidence of DSA in the form of serrations and a negative strain-rate dependency are also visible. The increase of strength by DSA is associated with a decrease in ductility. In the present case, the A50 tensile strain value has a global minimum of A80 = 16% at $T = 400^\circ\text{C}$.
- In the range $600^\circ\text{C} \leq T \leq 1000^\circ\text{C}$ the material is deforming under steady state creep condition. In this stage, the material exhibits no strain hardening and the strength decreases rapidly with increasing temperature.

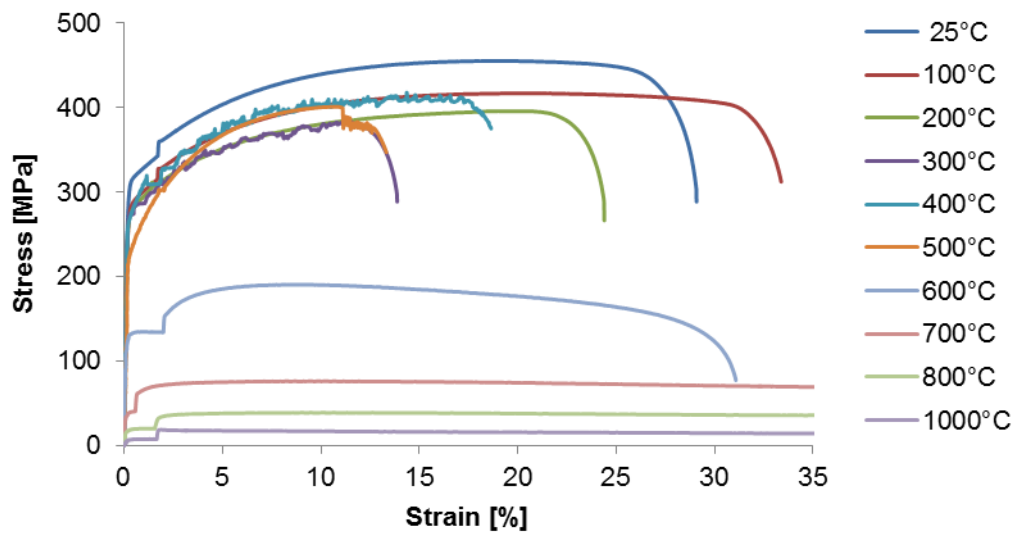


Figure 2 Stress - strain curves at different temperatures for steel 4016-2.

The steady state test results for the stabilized steel 4509-2 are shown in Fig. 3. From the figure, it can be seen that the effect of DSA is almost negligible for the stabilized material. Furthermore, the temperature range for steady state creep is translated to higher temperatures and starts at $T = 750^{\circ}\text{C}$. These observations are consistent with principles of physical metallurgy [7,8].

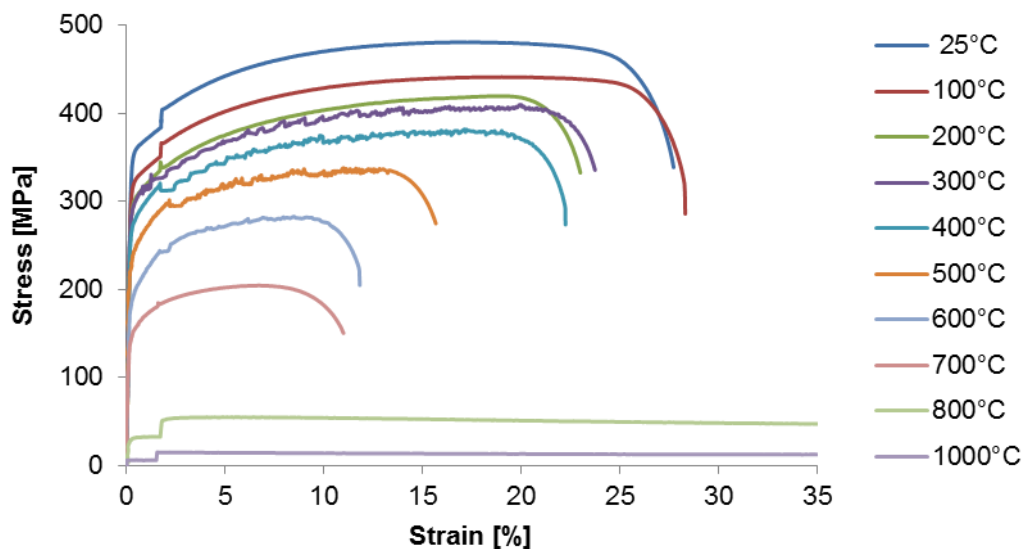


Figure 3-Stress- strain curves at different temperatures for steel 4509-2.

The reduction factors $k_{0.2,\theta}$ for 0.2% proof stress derived for all studied materials based on steady state test results are shown in Fig. 4. The reduction factor $k_{0.2,\theta}$ is defined as the 0.2% proof stress at elevated temperature normalized by the corresponding room temperature value. From the figure, it can be seen that the studied steels can be classified in two groups with similar characteristics. The first group contains the unstabilized grades 1.4003 and 1.4016 and the second group the stabilized steels 1.4509, 1.4521 and 1.4621. Inside both groups, the differences between grades and producers are insignificant. The same classification also applies to the ultimate strength reduction factor $k_{u,\theta}$ shown in Fig. 5. This reduction factor $k_{u,\theta}$ is defined as the ultimate strength at elevated temperature normalized by the corresponding room temperature value.

It is worth noting that the grade 1.4003 undergoes a phase transition from ferritic to austenitic state at approximately $T = 800^{\circ}\text{C}$. The phase transition is marked by a step in the reduction factor curves. Due to the phase transition, the strength of the material increases, and the work hardening capability is restored. The phase transition is associated with a volume decrease of approximately 1.0% and with a change in the coefficient of thermal expansion. These changes are often detrimental for the fire resistance of structural members.

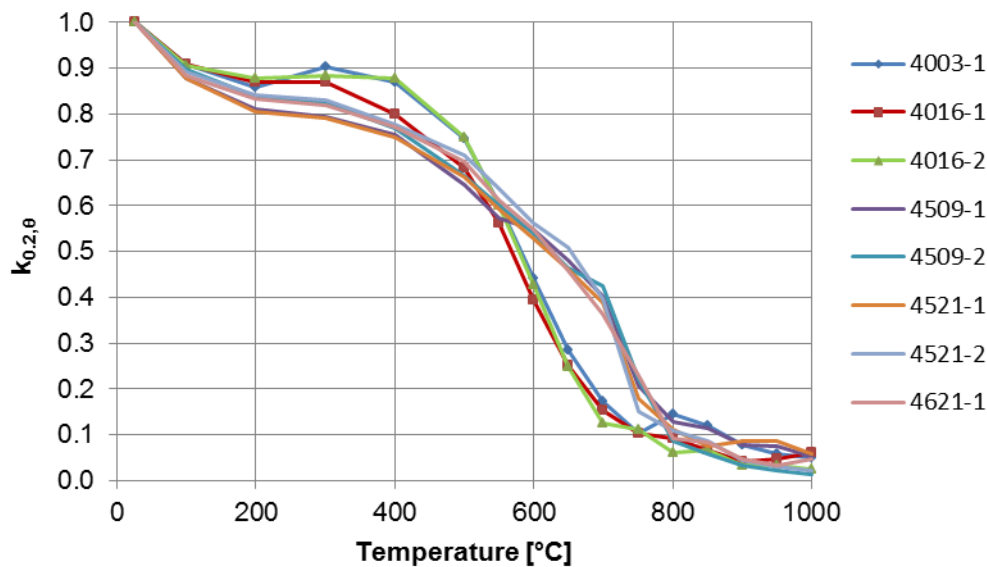


Figure 4 The 0.2% strength reduction factors derived from steady state tests.

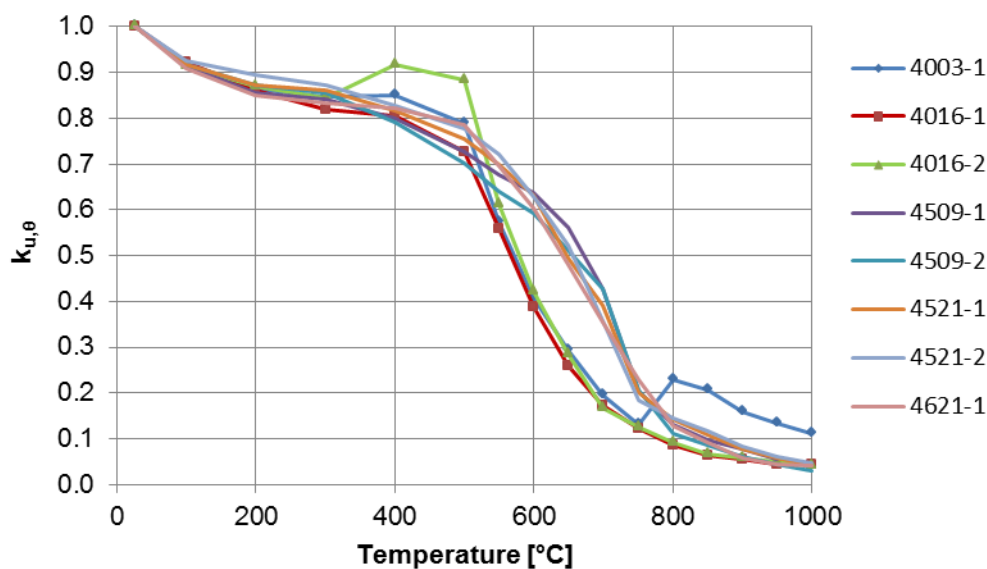


Figure 5 The ultimate strength reduction factors derived from steady state tests.

Degradation of elastic stiffness

The modulus of elasticity was determined as the slope of the linear-elastic part of the stress-strain curve. Accurate determination of the modulus of elasticity based on tensile test results is, however, difficult for a number of reasons [9]. On one hand, the linear-elastic part of the stress-strain curve is short for materials, which do not exhibit a clearly defined yield point. Therefore, inelastic effects such as creep and plastic yielding are influencing in the test results. The systematic error caused by the inelastic behaviour on the elastic modulus is always negative; creep and plasticity tend to decrease the slope of the curve rather than to increase it. On the other hand, even a small inaccuracy in the measured stress-strain response has a significant influence on the elastic modulus determined using the slope. Small error in the test setup such as a small initial curvature of test piece or a small misalignment of the specimen may have a remarkable influence on the obtained Young's modulus. Consequently, dispersion in the elastic modulus determined this way is typically large.

The elastic modulus values determined using the steady state test results for all studied steel are shown in Fig. 6. The dispersion in the elastic modulus values is remarkable. Due to the large dispersion, all measurements were treated as one set of data and a common reduction factor curve was derived for all studied grades. The data was fitted with a piecewise linear function. The result is shown in Fig. 7. The end-points of the line segments are given in Table 3. The standard error of the model is 0.14.

Table 3 Line segment end-points for elastic stiffness reduction factor.

Temperature (°C)	$k_{E,\theta}$
25	1.00
500	0.92
800	0.24
1000	0.084

The degradation of elastic stiffness in the present work is somewhat high compared to the values published by steel producers [10, 11]. The discrepancy becomes pronounced in the steady state creep domain, above $T = 600^\circ\text{C}$.

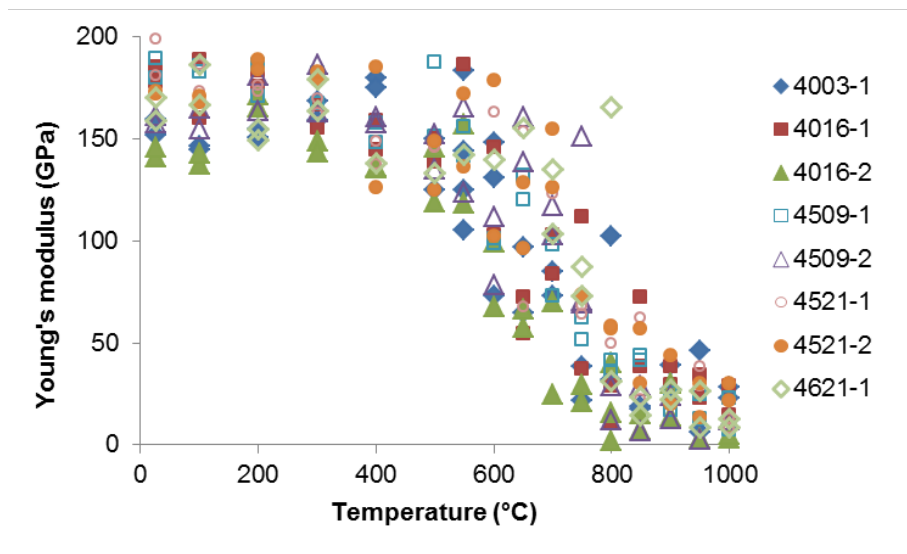


Figure 6 The scatter in the elastic modulus values was large

3.2 Transient State Test Results

Transient state tests were carried out on steels 4509-2 and 4521-3. The heating rate was $10^\circ\text{C}/\text{min}$. Sixteen different load levels between 10% and 90% of the yield stress were used. The thermal elongation was measured using a minimal load level of 3 MPa. The thermal elongation of steel 4521-2 is shown in Fig. 8. The obtained value for the linear coefficient of thermal expansion between room temperature and 100°C was $\alpha = 12.0 \cdot 10^{-6} (\text{°C})^{-1}$ and $\alpha = 11.2 \cdot 10^{-6} (\text{°C})^{-1}$ for steels 4509-2 and 4521-3, respectively.

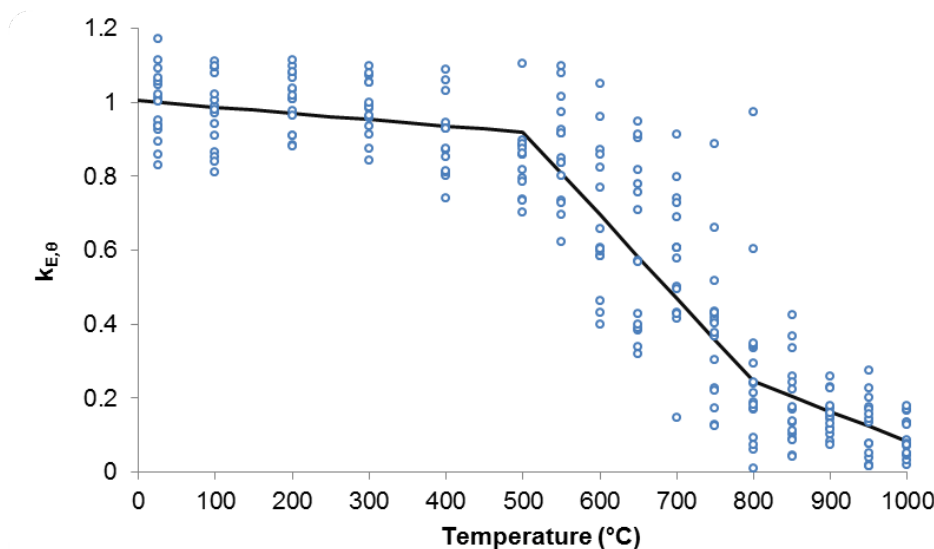


Figure 7 Modeled reduction factor for the elastic stiffness

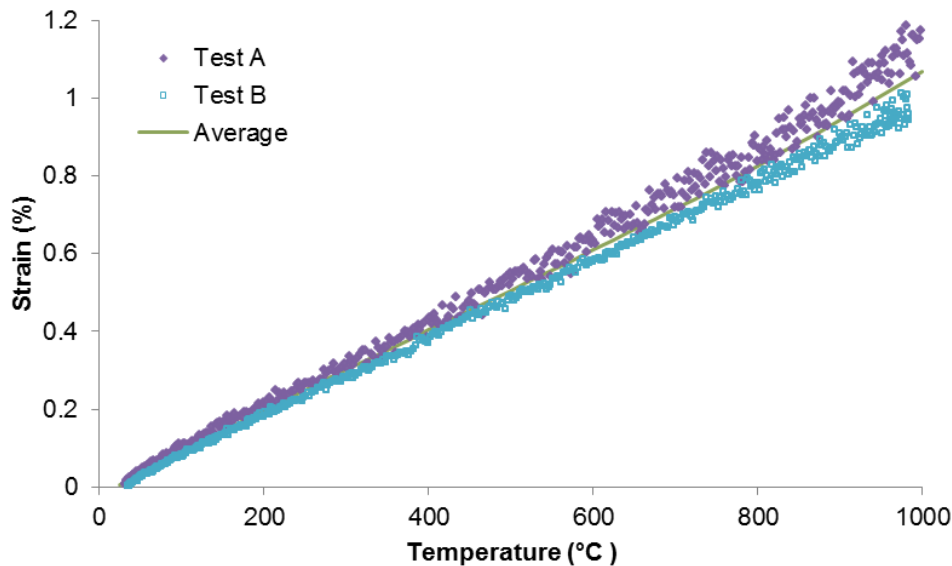


Figure 8 The thermal expansion for steel 4521-3

Figure 9 shows transient test results for steel 4521-3. The step-like feature on the left is repeatable and can be attributed to dynamic strain aging. The strength values corresponding to 0.2% plastic strain, 2.0% total strain and the ultimate tensile strength for both steels are shown in Figures 10 and 11. The results show that the strength is degrading rapidly as the temperature approaches $T = 800^{\circ}\text{C}$. Figures 12 and 13 compare the strength reduction factors obtained using both methods. It can be observed that there is good agreement between the two sets of reduction factors. The transient method gave slightly lower reduction factor values below $T = 700^{\circ}\text{C}$. Above this limit, i.e., in the steady state creep domain, the transient test method gave slightly higher values for the reduction factors.

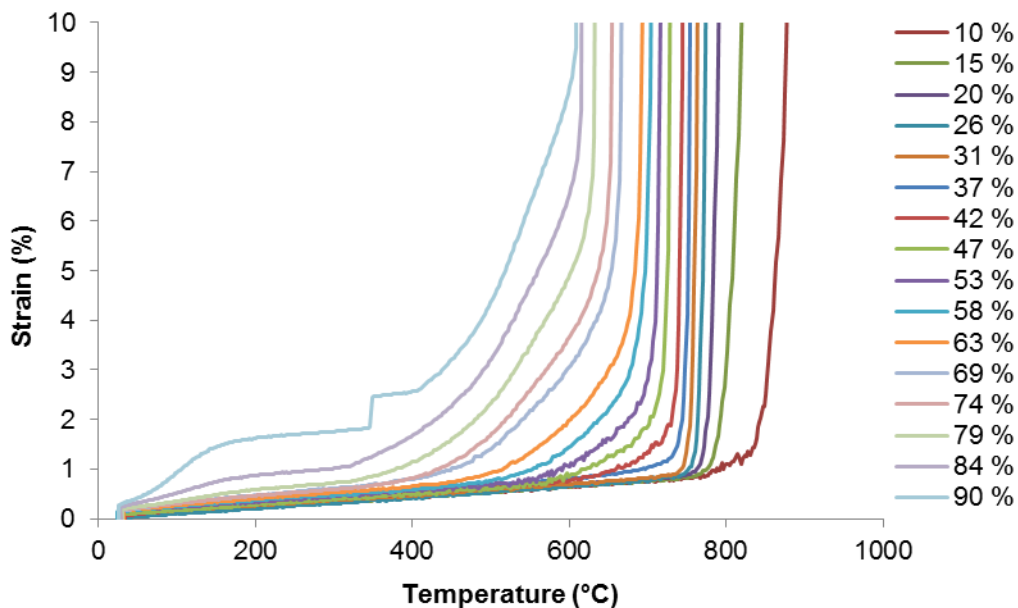


Figure 9 The transient test results measured for 4521-3. The strain includes the thermal expansion

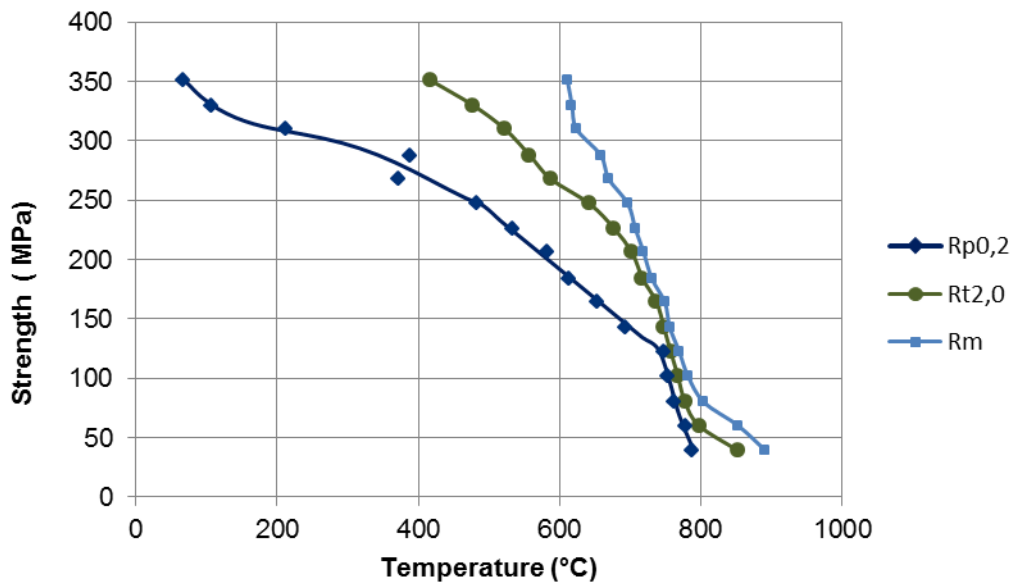


Figure 10 The stress values corresponding to 0.2% plastic strain, 2% total strain and the ultimate tensile strength for 4521-3.

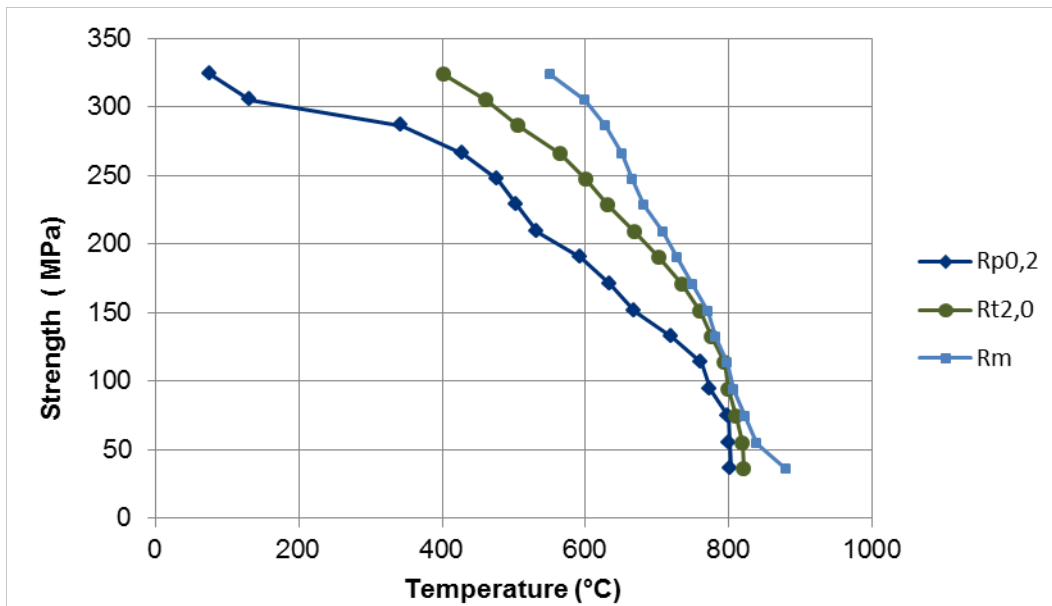


Figure 11 The stress values corresponding to 0.2% plastic strain, 2% total strain and the ultimate tensile strength for 4509-2.

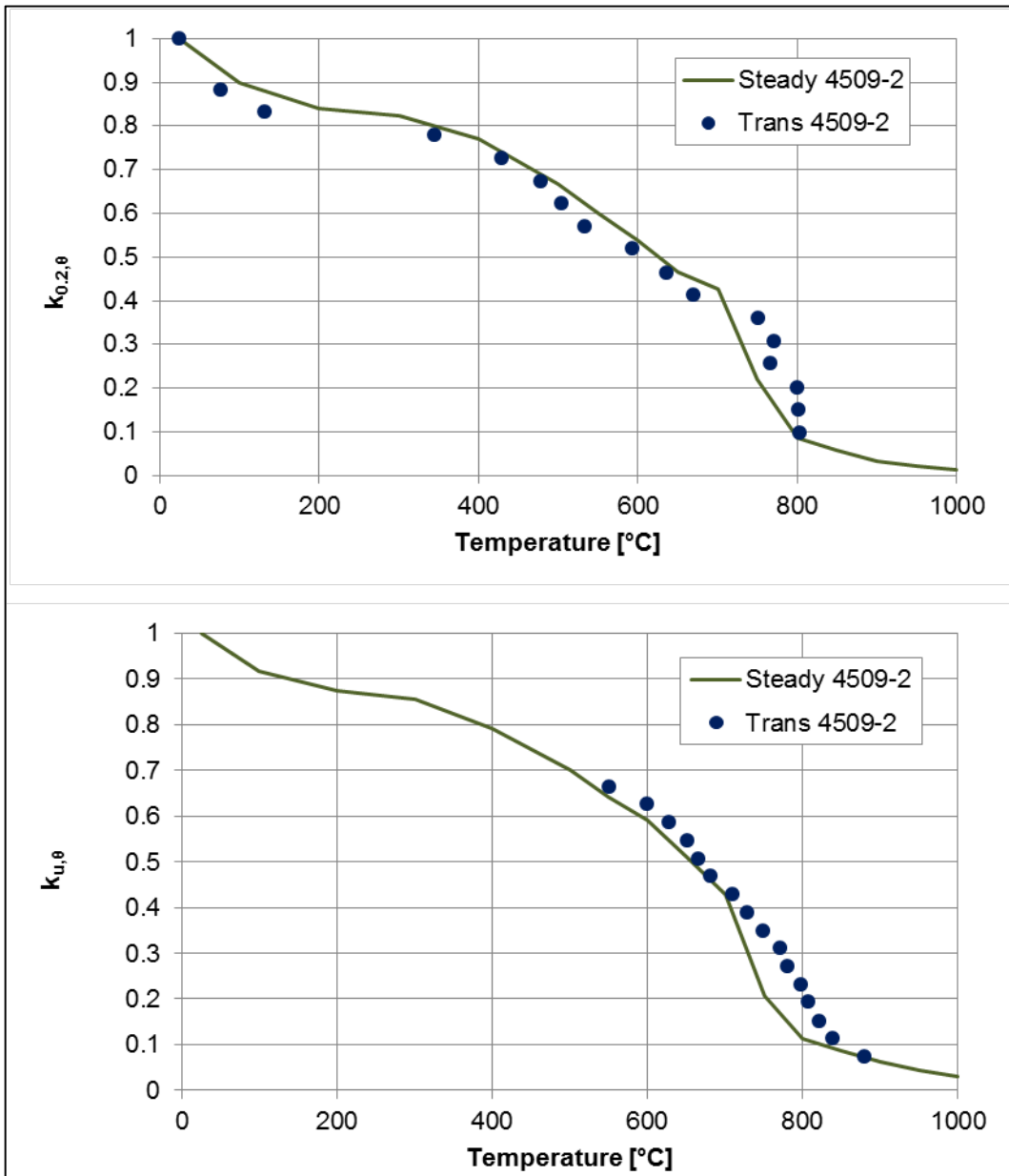


Figure 12 Reduction factors for 4509-2 obtained using the transient and steady state tests methods

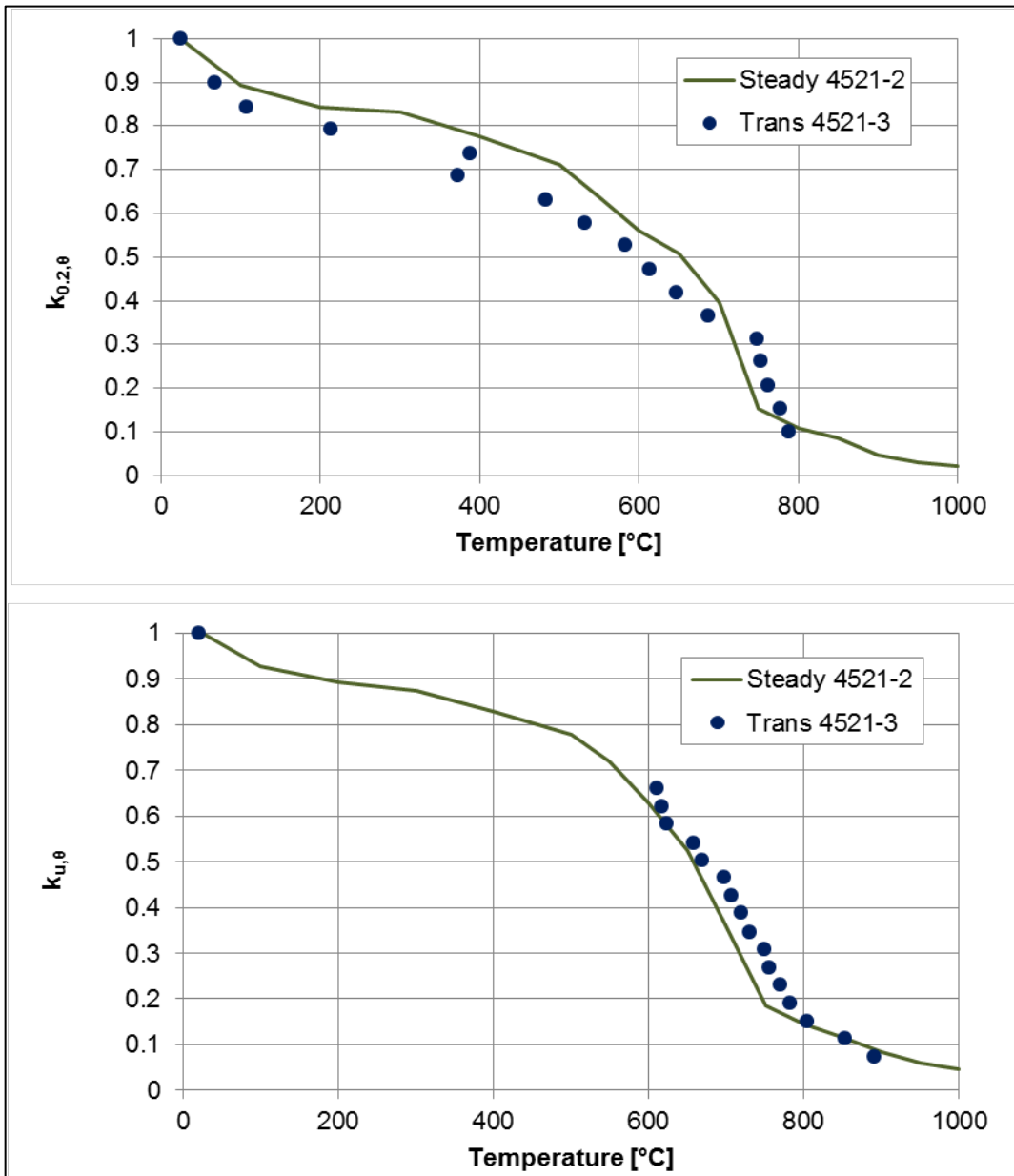


Figure 13 Reduction factors for two grade 1.4521 steels by the same supplier obtained using the transient and steady state tests methods

4 Design values

The experimental results suggest that the investigated ferritic stainless steels grades can be divided in two groups with similar characteristics in each group. The first group contains the unstabilized grades 1.4003 and 1.4016, and the second group contains the stabilized grades 1.4509, 1.4521 and 1.4621.

A combination of test results obtained in this work enables derivation of the fire design parameters for both groups of steels. Three design curves are needed for fire design of stainless steel structures: the reduction factor for the 0.2% proof strength $k_{0.2,\theta}$, the reduction factor for the ultimate tensile strength $k_{u,\theta}$, and the factor $k_{2\%,\theta}$. The factor $k_{2\%,\theta}$ determines the elevated temperature strength at 2% total strain $\sigma_{t2.0,\theta}$ by means of the 0.2% proof strength $\sigma_{0.2,\theta}$ and the ultimate tensile strength $\sigma_{u,\theta}$.

$$\sigma_{t2.0,\theta} = \sigma_{0.2,\theta} + k_{2\%,\theta}(\sigma_{u,\theta} - \sigma_{0.2,\theta}) \quad (2)$$

The reduction factors obtained in the present work for the first group steels, the unstabilized ferritic grades 1.4003 and 1.4016, are shown in Fig. 14. The values provided in EN 1993-1-2 for the grade 1.4003 are shown for comparison. The proposed values follow closely the values provided by EN 1993-1-2 for the grade 1.4003. The proposed values for the factor $k_{2,0}$ are shown in Fig. 15. The comparison between the proposed factor $k_{2,0}$ values and the values given in the EN 1993-1-2 for the grade 1.4003 is shown in Fig. 16. It can be observed that there is a small difference between the proposed values and the design values of EN 1993-1-2 between room temperature and $T = 300^\circ\text{C}$. This discrepancy is most likely caused by a difference in testing speed used for the $Rp_{0,2}$ and $Rt_{2,0}$ values. The experimental values for

Rp0,2 and Rt2,0 reported in the present work correspond to the same slow testing speed. However, additional room temperature tensile tests carried out on steel 4003-1 showed that the room-temperature value of $k_{2\%,\theta}$ factor increases from of $k_{2\%,\theta} = 0.28$ to $k_{2\%,\theta} = 0.38$ if the loading rate is changed before recording the Rt2,0 value, Table 4.

Table 4 Influence of loading rate on tensile test results at room temperature for steel 4003-1. The test method refers to the standard EN ISO 6892-1 and defines the loading rates used.

Test Method	Change of loading rate at	Rp0,2 N/mm ²	Rt2,0 N/mm ²	Rm N/mm ²	$k_{2\%,\theta}$
A222	-	333	379	483	0.31
A222	-	333	379	482	0.31
A224	$\epsilon = 1.5\%$	332	392	491	0.38
A224	$\epsilon = 1.5\%$	333	393	493	0.38
A224	$\epsilon = 3.0\%$	334	380	495	0.29
A224	$\epsilon = 3.0\%$	334	380	496	0.28

Fire design parameters for the second group of materials, the stabilized grades 1.4509, 1.4521 and 1.4621 were derived by combining the steady state and transient state test results shown above. The average of transient test results were used when available. The steady state results averages over tested steels were used to supplement the transient test results in the regions where the transient test results were not available. The derived values are shown in the Figures 17, 18 and 19.

The fire design factors proposed in the present work for the two groups of ferritic stainless steels are summarized in Tables 5 and 6. It is worth noting that the value of the factor $k_{2\%,\theta}$ could not be reliably determined throughout the whole temperature range. The steady state test results could be used only up to the beginning of the steady state creep deformation. The transient test results, on the other hand, could be used for calculating the values up to the point in which the strength curves become almost vertical.

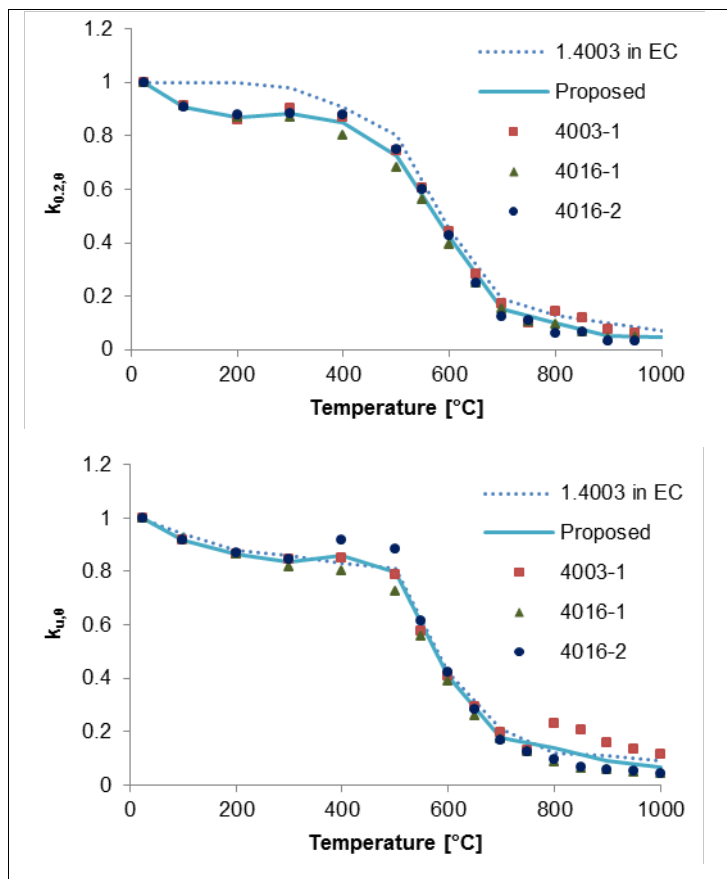


Figure 14 Reduction factors $k_{0.2,\theta}$ and $k_{u,\theta}$ derived in the present work for unstabilized grades, the values provided by EN 1993-1-2 for 1.4003 and test data

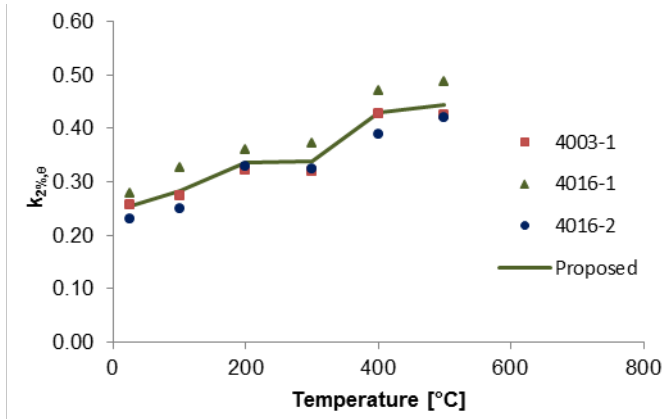


Figure 15 Factor $k_{2\%,\theta}$ derived for unstabilized grades and test data

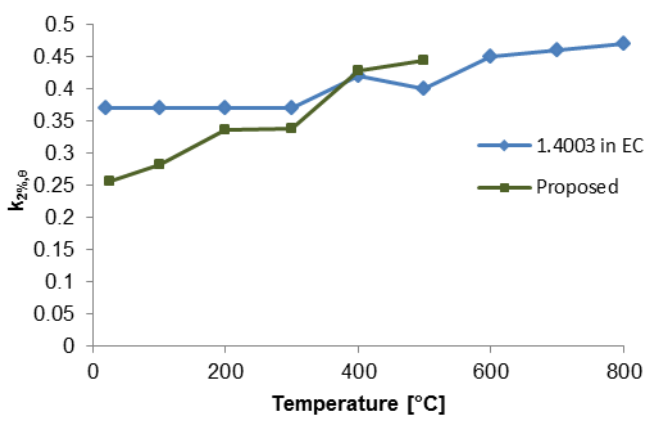


Figure 16 The proposed values of factor $k_{2\%,\theta}$ and the values provided by EN 1993-1-2 for 1.4003

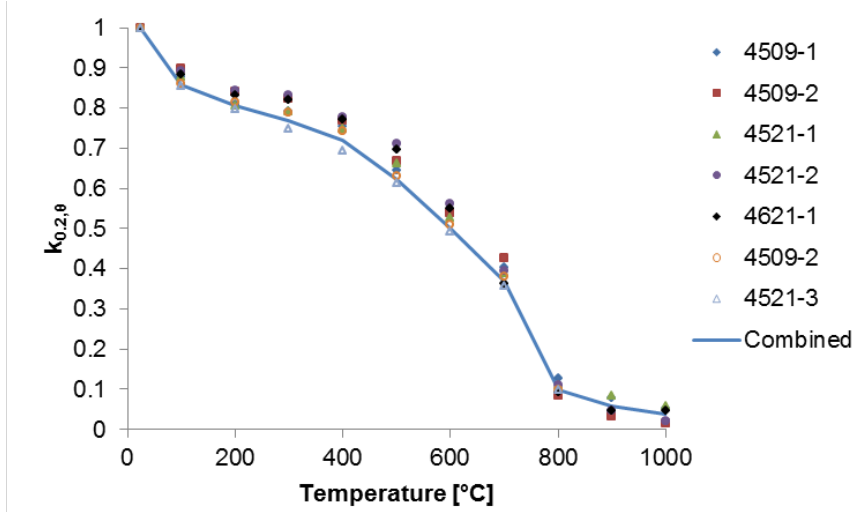


Figure 17 Reduction factor $k_{0.2,\theta}$ derived for stabilized grades and experimental data. The steady state test results are marked with filled symbols

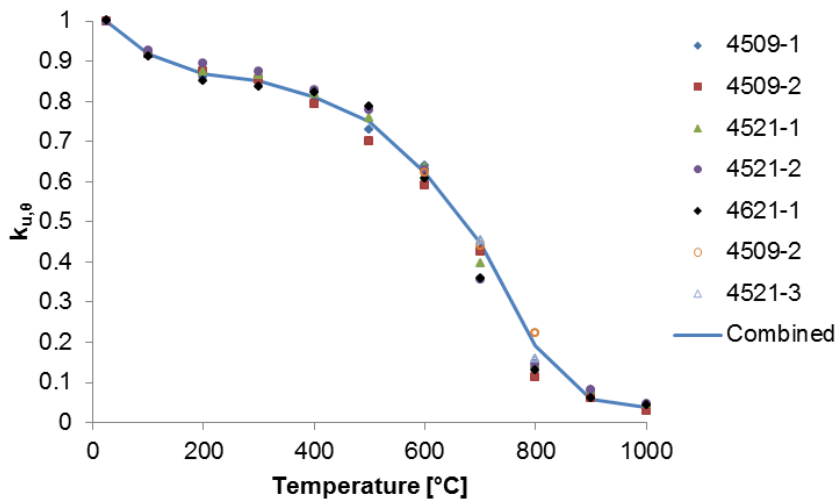


Figure 18. Reduction factor $k_{u,0}$ derived for stabilized ferritic grades and test data. The steady state test results are marked with filled symbols.

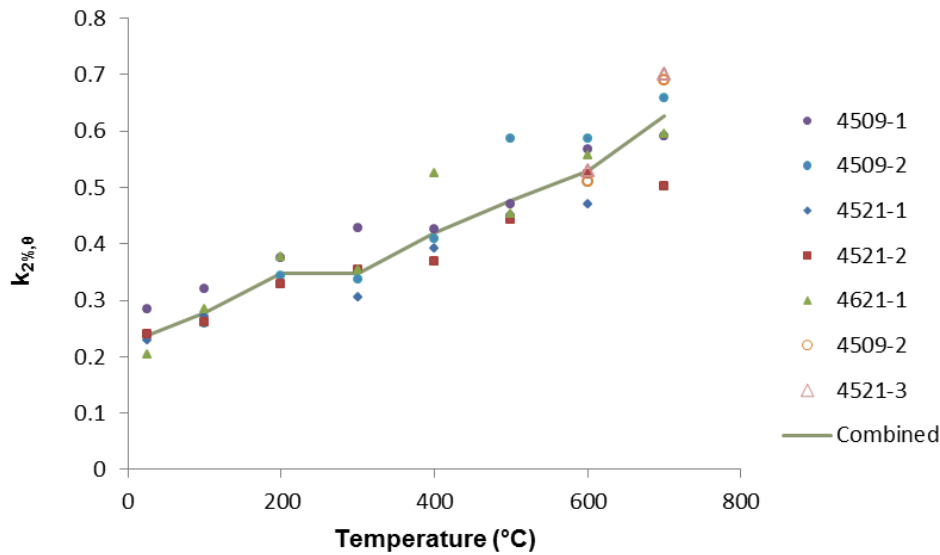


Figure 19. The derived factor $k_{2\%,0}$ for the stabilized grades and test data. The steady state test results are marked with filled symbols.

Table 5. Proposed fire design parameters for unstabilized ferritic grades 1.4003 and 1.4016.

Temperature (°C)	$k_{0,2,\theta}$	$k_{u,\theta}$	$k_{2\%,\theta}$
25	1.00	1.00	0.26
100	0.91	0.92	0.28
200	0.87	0.87	0.34
300	0.89	0.84	0.34
400	0.85	0.86	0.43
500	0.73	0.80	0.44
600	0.42	0.41	0.44
700.00	0.15	0.18	0.44
800.00	0.10	0.14	0.44
900.00	0.05	0.09	0.44
1000.00	0.05	0.07	0.44

Table 6. Proposed fire design parameters for the stabilized ferritic grades 1.4509, 1.4521 and 1.4621.

Temperature (°C)	$k_{0,2,\theta}$	$k_{u,\theta}$	$k_{2\%,\theta}$
25	1.00	1.00	0.24
100	0.86	0.92	0.28
200	0.81	0.87	0.35
300	0.77	0.85	0.35
400	0.72	0.81	0.42
500	0.62	0.75	0.48
600	0.50	0.62	0.53
700.00	0.37	0.45	0.63
800.00	0.10	0.19	0.63
900.00	0.06	0.06	0.63
1000.00	0.04	0.04	0.63

5 Summary and Conclusions

In the present work, an experimental research programme was carried out to investigate the mechanical properties of various ferritic stainless steels at temperatures up to 1000°C. The objective of the work was to derive the strength retention factors for ferritic stainless steel grades 1.4016, 1.4509, 1.4521 and 1.4621 in the temperature range between +20°C and +1000°C. Material from two European producers was used when available.

The results show that the ferritic stainless steel can be divided in two groups with similar characteristics in each group. The first group contains the unstabilized grades 1.4003 and 1.4016, and the second group contains the stabilized grades 1.4509, 1.4521 and 1.4621. The experimental test results obtained were used to derive fire design parameters for both groups.

Acknowledgements

The research leading to these results has received funding from the European Community's Research Fund for Coal and Steel (RFCS) under Grant Agreement no. RFSR-CT-2010-00026, Structural Applications of Ferritic Stainless Steels.

References

- [1] EN 1993-1-2. Eurocode 3: Design of steel structures Part 1.2: General rules - Structural fire design. CEN, 2005.
- [2] EN 1993-1-4. Eurocode 3. Design of steel structures: Part 1.4: General rules - Supplementary rules for stainless steels. CEN, 2006.
- [3] L. Gardner and N.R. Baddoo. Fire testing and design of stainless steel structures. *Journal of Constructional Steel Research*, 2006: 62: 532–543.
- [4] L. Gardner, A. Insausti, K.T. Ng and M. Ashraf. Elevated temperature material properties of stainless steel alloys. *Journal of Constructional Steel Research*, 2010: 66: 634 - 647.
- [5] J. Chen and B. Young. Stress–strain curves for stainless steel at elevated temperatures. *Engineering Structures*, 2006: 28: 229–239.
- [6] G. Roebben, B. Bollen, A. Brebels, J. Van Humbeeck and O. Van der Biest. Impulse excitation apparatus to measure resonant frequencies, elastic moduli, and internal friction at room and high temperature. *Review of Scientific Instruments*, 1997: 68: 4511 – 4515.
- [7] R. Abbaschian, L. Abbaschian and R. E. Reed-Hill, *Physical Metallurgy Principles*, 4th ed., Cengage Learning, Stamford, 2008.
- [8] R.E. Smallman and R.J. Bishop *Modern Physical Metallurgy*, 6th ed., Butterworth-Heinemann, Oxford, 1999.
- [9] J. D. Lord and R. M. Morrell. Elastic modulus measurement - obtaining reliable data from the tensile test. *Metrologia*, 2010: 47: S41–S49.
- [10] Product Data Bulletin for 11Cr-Cb Stainless Steel. AK Steel, West Chester, 2007.
- [11] Outokumpu Ferritic Stainless Steel Grades. Outokumpu, Avesta, 2012.